Emergency gate closing in a Kaplan turbine intake for runaway condition: CFD transient study for two-phase flow and experimental validation

Emergency gate closing in a Kaplan turbine intake for runaway condition: CFD transient study for two-phase flow and experimental validation

A Rivetti[1], G Angarita[2], M Angulo[1], F Botero[2], S Liscia[1]

[1] Laboratorio de Hidromecánica, Facultad de Ingeniería, Universidad Nacional de La Plata, 47 Nº 200, La Plata, Argentina.
[2] Mecánica Aplicada, Escuela de Ingeniería, Universidad EAFIT, Carrera 49 N° 7 Sur-50, Medellín, Colombia.

E-mail: arturorivetti@gmail.com

Abstract. In order to prevent a turbine to reach its runaway speed when load rejection occurs, an emergency closing system must be devised in case the regulation system fails. For Kaplan turbines, fixed wheel gates located in the turbine intake or in the draft tube outlet are usually employed. Gates of this type are move by gravity and the closing velocity is controlled by gantry cranes. The closing maneuver is complex due to the high flow rates inherent to runaway conditions and the rotational deceleration during the gate's closing time. Research on this topic is scarce and limited, and numerical studies are usually clouded by uncertainties concerning the setting of proper boundary conditions. In this work, the closing maneuver of the emergency fixed wheel gates at the intake of a Kaplan turbine was studied with CFD two-phase transient simulation. The software used was ANSYS CFX, that solves unsteady Navier-Stokes equations (URANS) by means of the finite volume method. The simulated domain includes a 2D case from one of the span of the semi-spiral casing and a 3D case of a complete span. Two types of simulation were considered, namely: quasi-steady state, where the position of the gate is fixed; and full transient state, where the gate movement was modelled by an immersed solid model. In search of the optimum model layout with its set of boundary conditions, numerical results were compared and validated against experiments performed on a physical scale model in accordance with IEC 60193 norms for several turbulence models. Results show that the pull-up force on the gate increases as it is being closed. Analysis of pressure fluctuation at different points of the gate suggest that the main frequency component is the vortex shedding of the gate lip.

1. Introduction

Given the risk they entail, runaway conditions are to be avoided, especially when operating at full head. Hydroelectric powerplants have thus to be provided with safety mechanisms of quick response that are able to protect the turbines by limiting their exposure to such flow conditions until their angular movement stops completely.

In case the primary shutdown system (i.e., distributor shutdown) fails, one emergency mechanism must be resorted to, namely shutting down a gate located either at the intake or at the draft tube of the turbine [1]. The forces that arise during the shutdown process and their oscillatory character are related mainly to the shape of the gate lip [2] and can be of such magnitude that might lead to the collapse of the gantry crane [1].

Kostecky et. al. [3] studied the hydrodynamic forces in an emergency gate with a flat bottom edge using a numerical tool based on the vortex method. They found that vortex detachment instabilities are

the main cause of vertical vibration in the gate. Sund and Magnusson [4] performed numerical simulations on a similar case for different bottom edge angles and closing velocities. The downpull force was shown to decrease for angles from 9° to 20°, and force fluctuations reach the minimum value at 30°.

In the present work, numerical simulations were carried out to study the vertical force in a flat gate with a bottom angle of 19°. Results were validated against physical model measurements at a scale of 1/29. Finally, a qualitative and quantitative analysis of numerical results were performed.

The case study concerns the Yacyretá 20-turbine hydroelectric powerplant, which is provided with a gantry crane for the operation of three lift gates, one for each of the vanes of the intake (Fig. 1). Shutdown proceeds under controlled conditions over a period of approximately eight minutes. The gates have an upstream seal and the dimensions (in meters) are 18.4 x 8.2 x 9.31, and a weight of 135 tons.

Figure 1: Front and side views of the gantry crane holding the intake emergency gates.

2. Methods and materials

2.1. Numerical simulation

The numerical simulation was implemented with the commercial software ANSYS CFX 2019 R2, which solves the Unsteady Reynolds Average Navier Stokes equations (URANS) using the finite volume method. For this case, several approaches were considered, starting with a 2D one-phase steady-state flow to a 3D two-phase fully transient flow. During the first steps of this study, the gate was considered static and was simulated for different positions. The movement of the gate was later considered with the aid of the immersed solid model available in CFX. This model involves two different independent meshes, namely, a background mesh, where the fluid flow takes place; and a solid mesh that can move and interact with the fluid. This model is not supported for two-phase simulations, where the density of the fluid is not constant. However, for this study, where the gate is always below the free surface and the water density can be assumed constant, simulations reach convergence and results were consistent with physical results.

Table 1. Simulated cases.

	Domain	Phases	Immerse solid model	Turbulence model
Steady state	2D	two-phase	No	SST
Transient	3D	two-phase	No	LES
Full Transient	2D	one-phase	yes	SST
		two-phase	yes	SST
	3D	one-phase	yes	LES
		two-phase	yes	LES

2.2. Computational domain

The computational domain includes one span of the semi-spiral casing (Fig. 2), i.e., only one gate is considered for the simulations. For 2D simulations, a slice of constant thickness in the *z* direction was considered. For the cases that include immerse solid model, the background domain is the part outlined in grey and the solid domain in black.

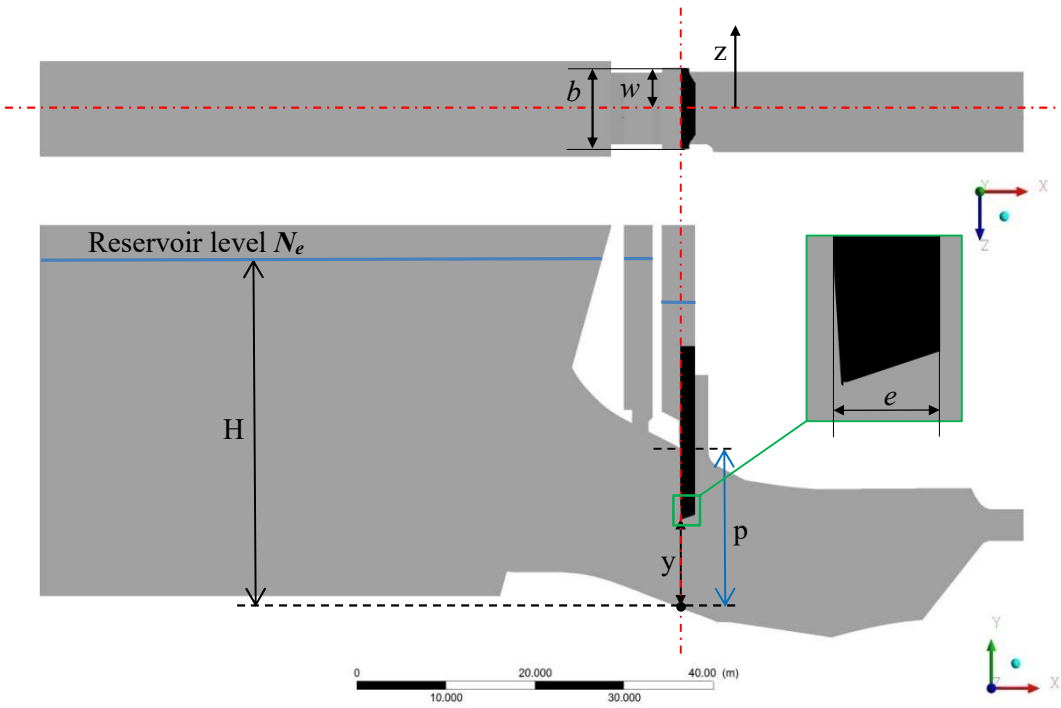

Figure 2: Plan (above) and side (below) views of the simulated 3D domain for one span of the semi-spiral casing.

2.2.1. Spatial discretization. Hexahedral-structural meshes were implemented for all cases. The software used was ICEM. For steady-state cases, where the immersed solid model was not used, the boundary layer was refined so as to obtain a suitable y+ value. For transient cases, where the gate is mobile, the boundary layer refinement was omitted. The final mesh was the result of the intersection of the background mesh and the solid mesh.

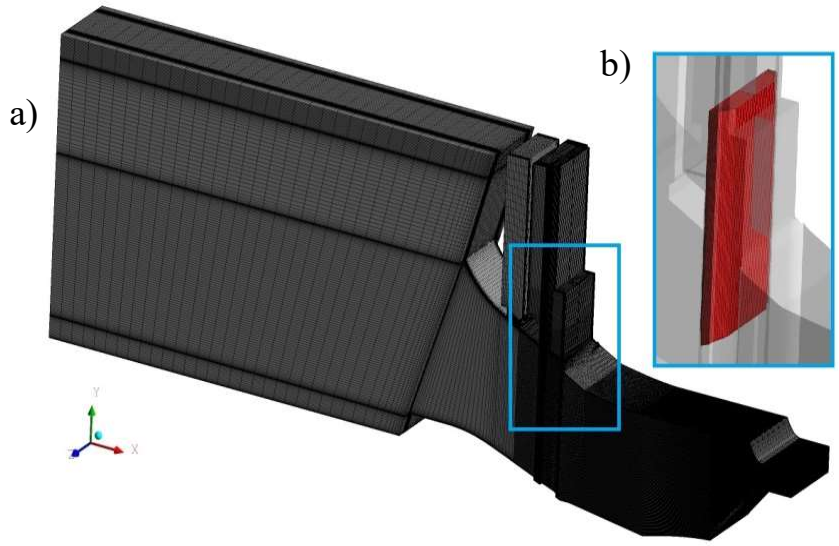

Figure. 3. Hexahedral structured mesh for the 3D case with the immerse solid model (right); (a) background mesh in gray; (b) Solid mesh in red.

Boundary conditions and numerical setup. Boundary conditions were chosen in order to reproduce the closing gate maneuver. The maximum flow rate, when the gate is fully open, corresponds to runaway at of-cam condition. The flow rate in function of gate opening was obtained from physical model experiments [6]. At the inlet, normal velocity was chosen with a value of $Q(y/p)/\Omega_{inlet}$. The reference pressure was set at one atmosphere. At the outlet, an Average Static Pressure was considered. Several simulations were performed at full gate opening in order to obtain an appropriate value of relative pressure at the outlet. In two-phase cases, the volume fraction of water was set to one under reservoir level and zero above as initial condition. Time step was set at 3.0E-4*$\Delta t/t_c$, where t_c is the closing time.

Model tests. Experiments were performed at the Laboratory of Hydromechanics of the National University of La Plata, Argentina. A test rig was used that consists in a closed circuit that allows for the testing of Kaplan and Francis turbines in compliance with IEC 60193 norm [5]. The scale model is a full Kaplan turbine including all its components: semi-spiral casing, stay and guide vanes, runner and draft tube. The gates are located in the semi-spiral casing inlet (Fig 4). Each gate was equipped with pressure sensors both at the top and at the bottom surfaces of the gate. Measured pressure is integrated over the gate to obtain the vertical force Fy. Flow rates were measured with a Venturi flow-meter within an error of 0.1%. More detailed information about the experimental setup is available in [6].

Figure 4. Intake with emergency gates of the Kaplan model turbine as mounted on the test rig.

2.3. *Data processing.* For the characterization of the forces acting on the gate, the dimensionless coefficient K_v and K_h are used (Eq. 1). The pressure was analysed in terms of the coefficient C_p, (Eq. 3).

$$K_v = \frac{D_p}{\gamma_w e\, b\, H}, \qquad K_H = \frac{F_x}{\gamma_w e\, b\, H} \tag{1}$$

Where Dp = downpull force, calculated as in Eq. 2, Fx = horizontal force on the gate, γ_w = water specific weight, e = gate width, b = gate depth, H = hydraulic head at the bottom inlet upstream the gate.

$$D_p = F_B - F_T - F_{Gw} \tag{2}$$

Where F_B = vertical force at the bottom of the gate, F_T = vertical force at the top of the gate, F_{Gw} = buoyancy force in the gate. If flow is zero then, $F_B - F_T = F_{Gw}$ and $D_p = 0$.

$$Cp = \frac{p_i - \tilde{p}}{\gamma_w (N_e - N_r)} \tag{3}$$

Where Cp = pressure coefficient, p_i = local pressure at a specified location, $\tilde{p}$ = mean pressure around the gate, N_e = reservoir water level, N_r = tail-water level.

3. Results

Downpull coefficient and CFD validation: Fig. 5 shows the downpull coefficient for scale model experiments and CFD simulations. The K_v coefficient is negative for almost the entire range of openings. For gate openings ranging from 1 to 0.5, K_v remains constant except for the range of 0.9-1, where positive values show up both for experiments and numerical results. For openings less than 0.5 K_v decreases exponentially down to values between -0.03 and -0.04. Divergences observed between experiments and numerical simulations in the range of openings between 0.25 and 0.4 can be attributed to the former being carried out for fixed gate positions whereas the latter were performed under the assumption of full transient flow (mobile gate). For openings greater than 1 (i.e., with the gate not yet lowered below the top of the vane), K_v equals approximately -1.0E-3, due to the water resistance to the movement of the gate.

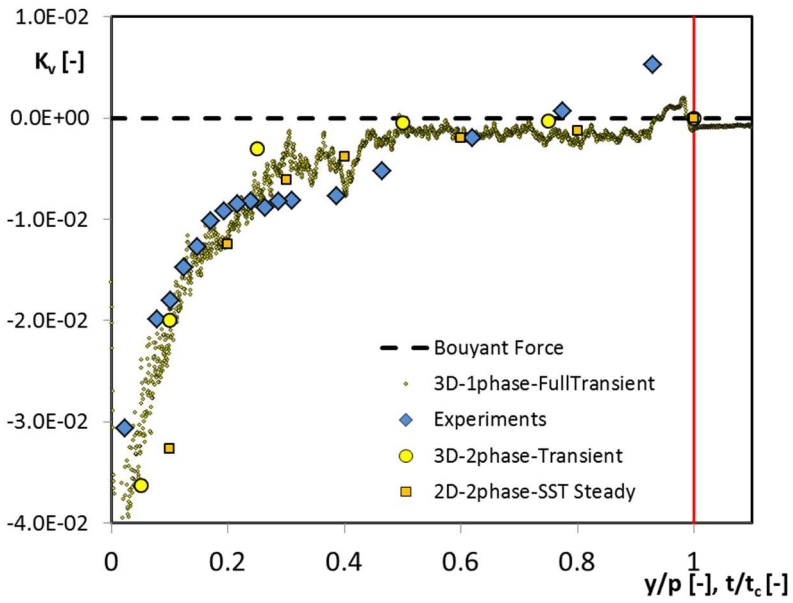

Figure 5. Downpull coefficient vs. gate opening (y/p) and time (t/t_c) for scale model experiments and CFD simulations. In dash black line (K_v=0) buoyancy force is represented. Positives values of K_v represent a downpull force and negatives values an uplift force.

Pressure distribution on the gate: The downpull force is the result of the integration of pressure on the gate times its horizontal projected area. Fig. 6 shows the pressure distribution coefficient, C_P, at the top and bottom surfaces for various gate openings and spanwise locations. The black line, which represents the hydrostatic conditions (flow rate Q = 0 and D_P = 0), is shown for reference. Fig. 6a) shows that, as the gate is lowered, pressure increases at the upstream part of the bottom surface above hydrostatic values resulting in negatives values for D_P, since pressure distribution remains hydrostatic on the rest of the surface. Fig. 6b) shows that the pressure distribution is essentially constant for the whole width of the gate. Fig. 6c) shows a strong variation of pressure coefficient near the span wall.

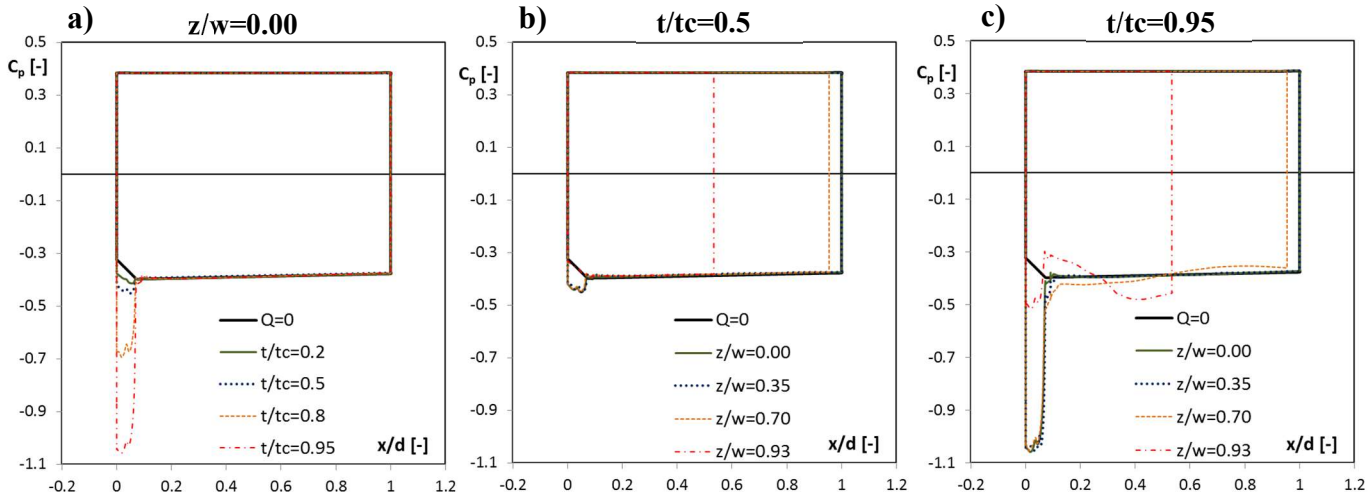

Figure 6. Variation of pressure distribution coefficient C_P around the gate for top surface (positive values) and bottom surface (negative values). a) Different gate apertures. b) and c) Constant gate opening and different spanwise positions.

The horizontal force on the gate is shown in Fig. 7a) expressed in terms of K_H. At full opening, both vertical upstream and downstream faces, are subjected to the same hydrostatic pressure profile, therefore K_H is zero (black dashed line). As the gate is lowered down into the vane, the mean pressure drops downstream the gate due to the energy loss, J. Therefore, the horizontal force becomes Ω_y*J. When the gate is fully closed, J is equal to the water level difference between the reservoir and tailwater level, N_e-N_r (blue dashed line). Fig. 7b) shows the downpull coefficient as calculated from K_H and as obtained from Dp. The strong correlation shows that the main part of the vertical force for this case is due to the presence of the upstream bottom angle.

$$K_v^* = K_H * \frac{\Omega_x}{\Omega_y} \quad (4)$$

Where K_v^* = downpull coefficient deduced from horizontal force, K_H = horizontal force coefficient, Ω_x = projected horizontal area of the upstream gate surface, Ω_y = vertical projected area of the gate.

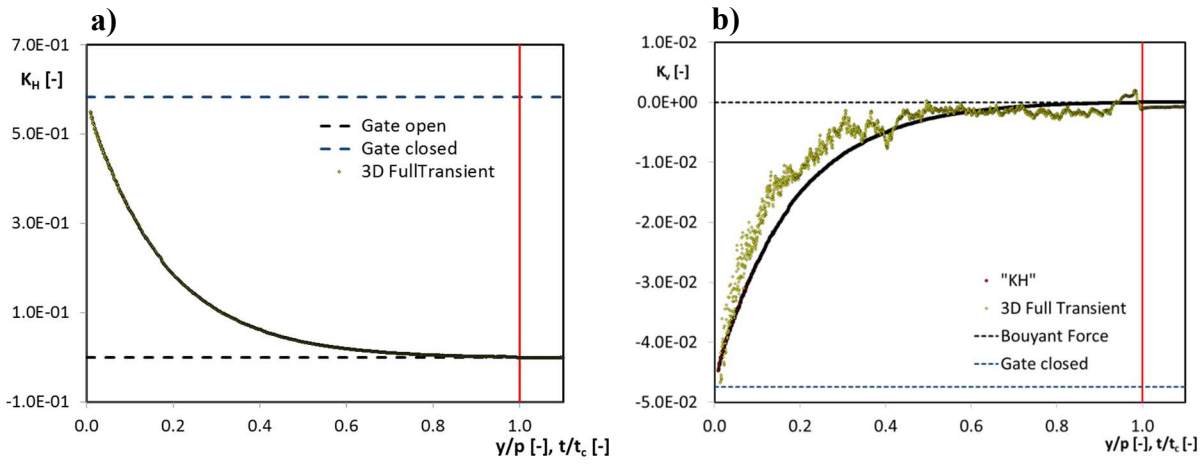

Figure 7. a) Force coefficient. b) Comparison between downpull coefficient K_v calculated and deduce from K_H.

Fig. 8 shows along the vertical plane that contains the center of the span ($z=0$). Pressure distribution patterns show a strong influence of gravity. Only in the contracted region near the gate lip, where high velocities arise, is a distortion of the hydrostatic distribution noticed. For an opening of y/d = 0.95, the pressure difference between the upstream and downstream sides of the gate are due to the hydraulic energy loss caused by the flow through the gate. Fig. 8c) shows the z-component of vorticity. The high velocity gradient produced downstream the gate lip generates vortex detachments that interact, splitting into smaller vortices with a macro circulation (indicated with a white arrow).

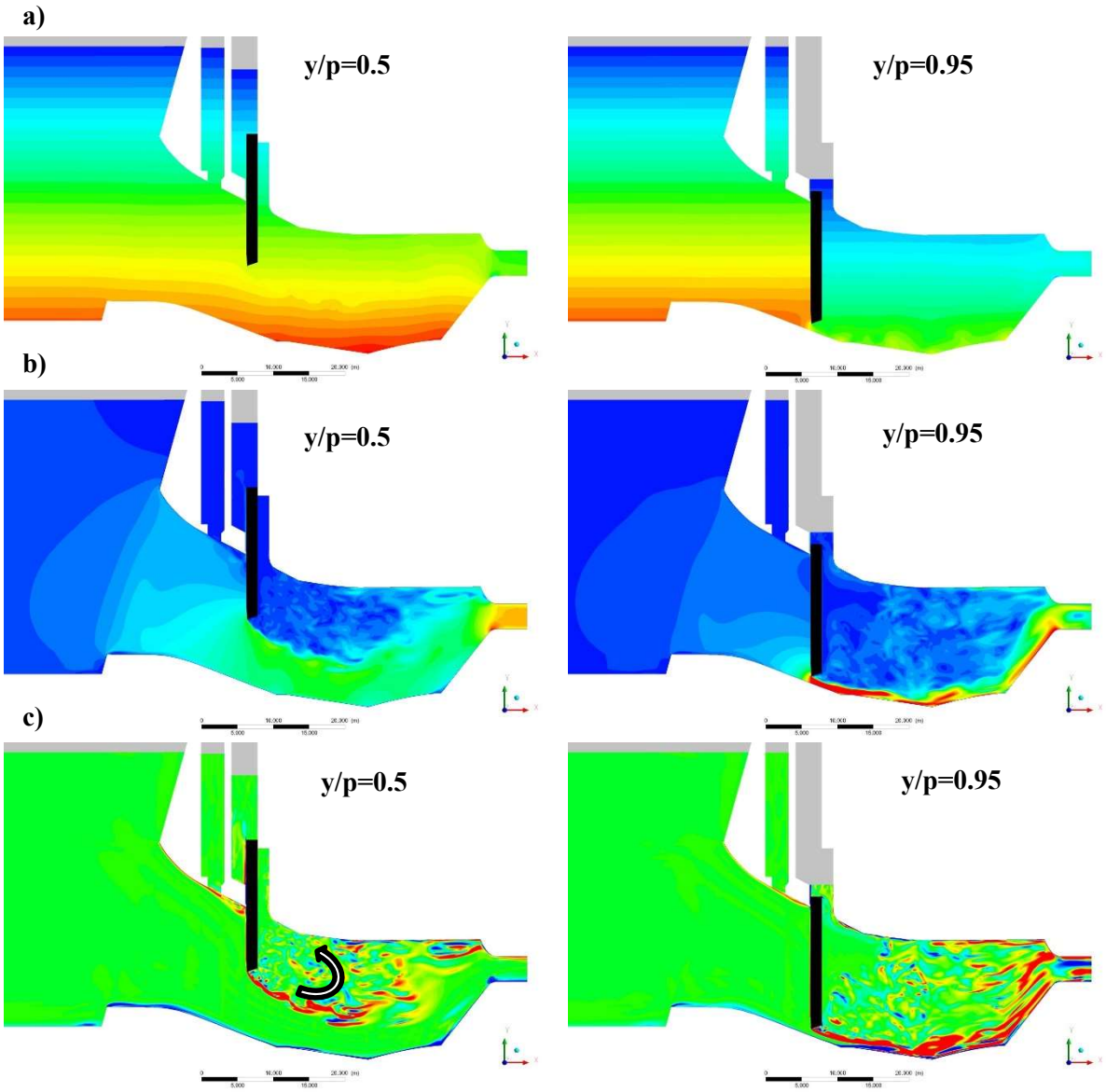

Figure 8: Flow visualization in the spanwise direction for *z/w*=0 and gates opening of 0.5 and 0.95 expressed as *y/p*. a) Pressure distribution. b) Velocity module. c) Vorticity in *z* direction.

4. Discussion

The hydrodynamic effects caused by the closure of the gate were found to cause uplift forces on the gate for all simulated cases. As its upstream face is slightly slanted (5 degrees with respect to the vertical direction), the hydrostatic imbalance between the gate's upstream and downstream sides would, by itself, explain such uplift forces. It would also help explain the disagreement between the results found herein with respect to those reported by Sund and Magnusson [4] (Fig. 9), on experiments with flat gates.

On the other hand, such slanted surface, along with the overhang lip, both reduce the effect of separation from the downstream face, thus decreasing the suction exerted on it. As a consequence, the downpull component that arises barely diminishes the magnitude of the uplift force (Fig. 10).

Two main frequencies components were detected both in pressure fluctuation at points located on the downstream face and the vertical force *Dp*. The highest one is related to the vortex detachment from the gate lip and has a Strouhal number of ~1.1, in agreement with results reported elsewhere [3]. This value remains roughly constant for all gate openings simulated. The second frequency component is due to the circulation downstream the gate, that forms large vortical structures. The Strouhal number for this mechanism is more variable, ranging between 0.03 and 0.09.

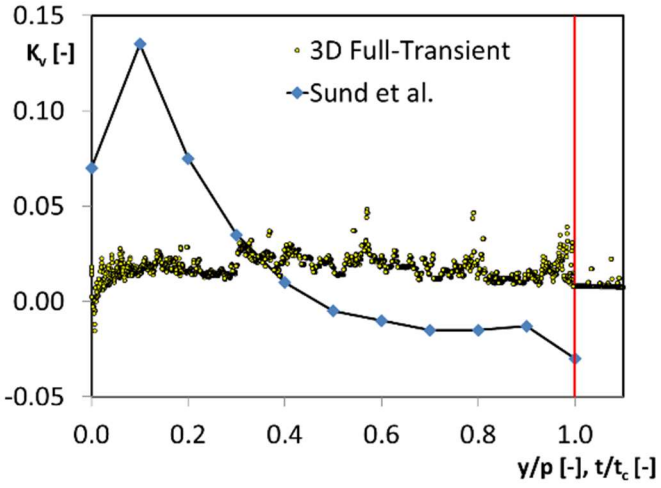

Figure 9: Downpull coefficient K_v without considering the vertical force component F_{B1} compared with the values obtained by Sund et al. [4].

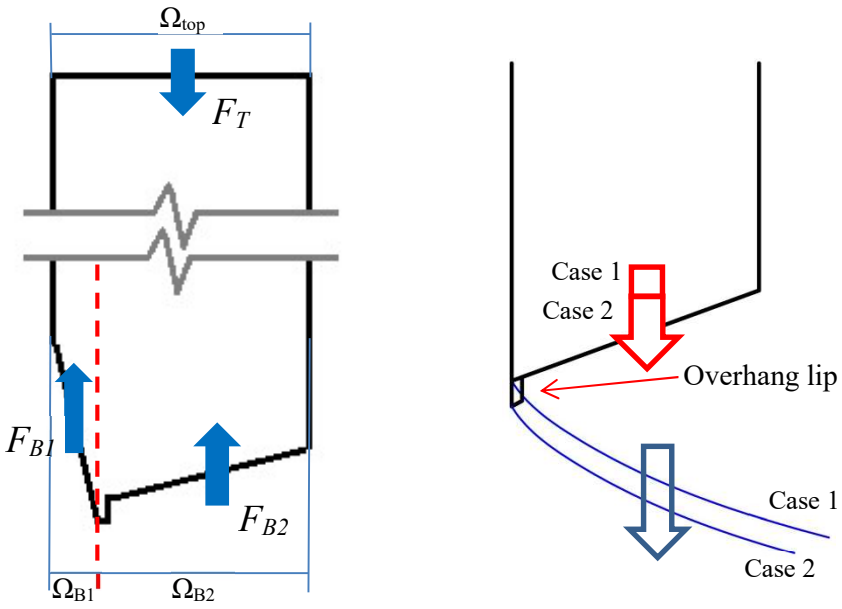

Figure 10: Left, vertical forces involved in the dawnpull coefficient. Right, decrease in the suction effect by the overhang lip.

5. Conclusions

A series of CFD simulations were carried out in a single span from a Kaplan turbine semi-spiral casing, including the emergency gate, with the aim of studying the hydrodynamic forces during closing maneuver.

The vertical force exerted upwards on the gate by the flow passage was seen to increase as the gate was lowered, reaching the maximum value when the gate is fully closed. This is explained mainly by the hydrostatic pressure distribution on both sides of the gate, whereas turbulent and flow separation effects appear to be of little relevance. Results cannot be directly extrapolated to other geometries, however, as seen in previous studies.

Results show a good agreement with experiments performed in a scale model, where the vertical force on the gate was obtained by integrating pressure points located along the gate. In the frequency domain, two main components were detected both in the vertical force on the gate and the pressure points in the downstream surface. The first one has a Strouhal number of ~1.1 and is due to vortex detachment from the gate lip, and the second one is caused by a large scale vorticity downstream the gate and has a Strouhal number of 0.03 to 0.09.

Acknowledgement

The authors would like to thanks to the technical director of the Yacyretá power station, Eng. Marcelo Cardinalli, for his kind permission to publish this work.

References

[1] Erbisti O 2014 *Design of Hydraulic Gates* (London: Taylor & Francis Group)
[2] Lewin J 2001 *Hydraulic Gates and Valves – In Free Surface Flow and Submerged Outlets* (Londres: Thomas Telford Ltd, London)
[3] Kostecki SW, 2011 Numerical analysis of hydrodynamic forcesdue to flow instability at lift gate, Archives of civil and mechanical engineering, Vol XI.
[4] Sund M, Magnusson F 2014 Numerical study on hydraulic vertical lift gate during shutdown process (Sweden: KTH Royal Institute of Technology School of Engineering Sciences)
[5] IEC standars 1999 *Hydraulic Turbines, Storage Pumps and Pump-Turbines-Model Acceptance Tests*; IEC 60193
[6] Angulo M, 2020, Emergency gates – model scale test at turbune runaway condition. 30th IAHR Symposium on Hydrauli Machinery and Systems. Lausanne Switzerland.